Evidence of Deep DOC Enrichment *via* Particle Export Beneath Subarctic and Northern Subtropical Fronts in the North Pacific

Chelsea Nicole Lopez* and Dennis Arthur Hansell

Department of Ocean Sciences, Rosenstiel School of Marine and Atmospheric Science, University of Miami, Miami, FL, United States

Here we provide compelling evidence that deep particle export enhanced dissolved organic carbon (DOC) concentrations beneath the Pacific's Subarctic Front (*SA*, ~42°N) and Northern Subtropical Front (*NST*, ~34°N). We report three main findings: First, deep export of subjectively small particles (128–512 μm) was apparent throughout the frontal zone in which the *SA* resides. However, export of large particles was specifically associated with the *SA*, rather than the entire frontal zone, and appeared to exclusively transfer DOC into the bathypelagic water column. Second, a similar DOC enrichment existed beneath the *NST*, though this signal was curiously not accompanied by observable particles (>128 μm). We conclude that export occurring previously in winter left this DOC behind as a residue, though the associated particles were no longer present by spring. Third, the presence of strong hydrographic fronts was not the only control on export that resulted in these unique DOC distributions. Deep export and DOC enrichment was also controlled by latitude-specific biogeochemical and hydrographic conditions, such as depth of the nutricline and seasonal mixed layer shoaling. Given these observations, the fronts within the transitional region of the North Pacific are clearly special locations for deep carbon sequestration and for providing uncommon DOC enrichment that ultimately supports the deep microbial community.

Keywords: dissolved organic carbon, export, North Pacific fronts, biogeochemistry, particle export, subtropical fronts, subarctic fronts

INTRODUCTION

Hydrographic frontal zones, given their complex physical dynamics, stimulate biological growth and particle export to the interior ocean (Roden, 1991; D'Asaro et al., 2011; Guidi et al., 2012; Juranek et al., 2012; Ohman et al., 2012). Exported particles release dissolved organic carbon (DOC) into the deep water column, a crucial process for sustaining the bathypelagic microbial community (Nagata et al., 2000, 2010) who mediate carbon sequestration. Bathypelagic bacterioplankton are abundant where overlying waters are most productive (Nagata et al., 2000; Hansell and Ducklow, 2003) and intrinsically where export is highest. Through respiration, these microbes convert DOC to inorganic forms, effectively sequestering carbon until

subsequent ventilation. However, the transformation of sinking particles to DOC to support these microbes is largely inferred rather than observed. In environments where export is minimal, DOC released at depth is likely rapidly consumed and an enrichment of DOC above typical background concentrations would unlikely be detected. Such may not be the case in high-export environments, as deep DOC enrichment was evident during strong bloom events in the Gulf of Alaska (Lopez et al., 2020). Given that enhancement of export has been associated with fronts (Ohman et al., 2012; Stukel et al., 2017), DOC surplus may be found in the bathypelagic waters beneath them as well. To explore this possibility, we present novel observations beneath well-defined, productive frontal zones in the central North Pacific. We first compare the distribution of DOC from 500 m to the seafloor to particle abundances segregated by size class. We then investigate the frontal zone distribution of surface nitrate, the depth of the nitracline, seasonal mixed layer depths (MLDs), and seasonal expansion/contraction of eutrophic conditions to understand controls on export. With this, we further our understanding of the codependence of front-derived mixing and the biogeochemical environment required for stimulating deep export leading to the enrichment of DOC.

Past work has explored upper ocean biogeochemical dynamics of fronts, alluding to the potential for deep export (Juranek et al., 2012; Lockwood et al., 2012; Ohman et al., 2012; Howell et al., 2017). Though little such work has been done on North Pacific frontal zones, one study revealed net community production to be elevated in the northern transition zone (Lockwood et al., 2012). In a front within the nearby California Current system, gravitational particle flux due to physical subduction beneath the mixed layer was 2–3× higher than neighboring water (Stukel et al., 2017) and up to 10× higher phytoplankton biomass was present where wind-driven frontal mixing could reach the nutricline (Whitt et al., 2017). In addition, fronts commonly host larger marine life that produce large detrital particles (Ohman et al., 2012; Kobari et al., 2020) capable of reaching great depth before being remineralized by the microbial community (Pearcy, 1991; Woodson and Litvin, 2015). Large particles have significant implications for the addition of DOC into the deep ocean, as they are preferentially remineralized by microbes that mediate DOC release (Smith et al., 1992) via disaggregation and solubilization (Alldredge et al., 1990; Smith et al., 1992).

Though the frontal zones in the transitional region of the North Pacific were identified four decades ago (Roden, 1980), and are physically well-characterized (Roden, 1991; Yuan and Talley, 1996), studies of their influence on DOC addition via carbon export are non-existent. From this work, we aim to better understand the following questions:

(1) Does enhanced particle export at these North Pacific fronts support bathypelagic DOC enrichment?
(2) If so, how do hydrographic and biogeochemical conditions in the upper layers of the frontal zones influence that export?

By exploring these questions, we move toward a better understanding of the role of frontal zones in broad scale processes, such as deep carbon sequestration and sustenance of bathypelagic microbes.

HYDROGRAPHIC CONTEXT: FRONTAL ZONES IN THE CENTRAL NORTH PACIFIC

We identified the location of frontal zones and their embedded fronts, well-known from previous studies, using hydrographic data from U.S. Global Ocean Ship-Based Hydrographic Investigations Program (GO-SHIP) section P16N occupied in 2015 (see "Data Availability Statement"), with consideration of isohaline structures described previously (Roden, 1970, 1980, 1981, 1991; Yuan and Talley, 1996). Density is not a useful tracer of fronts in this area due to temperature-salinity compensation at higher latitudes; further, salinity and temperature fronts do not always coexist (Roden, 1991), therefore we used salinity gradients to characterize the region.

The Subarctic–Subtropical Transition Zone (**Figure 1A**) separates the eutrophic, cyclonic subarctic and oligotrophic, and anti-cyclonic subtropical gyres (**Figure 1B**), being characterized by a gradual northward decrease in upper-ocean salinity (**Figure 2A**; ∼35–38°N). At the borders of this zone lie the **Subarctic Frontal Zone (SAFZ)** to the north and the **Subtropical Frontal Zone (STFZ)** to the south (**Figure 1A**), both formed by large-scale ocean circulation and air-sea heat exchange (Roden, 1991). In addition to fronts, mesoscale physical perturbations in these zones are common, consisting of temporally variable features such as eddies and jets (Käse et al., 1985; Roden, 1991; Nakamura et al., 2008).

The **SAFZ** marks the location for cold, low-salinity subarctic water subduction beneath warmer, higher-salinity water within the transition zone. Here it is located between the 33.0 and 34.1 isohalines (∼38–45°N; **Figure 2A**). The salinity gradients at the northern border of the **SAFZ** are characteristically less pronounced than at the southern border where the subarctic halocline outcrops, therefore we subjectively identified its location based upon Roden's past reports (Roden, 1970). In contrast, the **STFZ** is a high salinity feature spanning ∼30–35°N, bordered here by the 35.2 and 34.4 isohalines. These two systems zonally span much of the North Pacific without substantially deviating from their climatological positions (Yuan and Talley, 1996).

Prominent quasi-permanent fronts are embedded within these frontal zones. Within the **STFZ** lies the *Northern Subtropical Front* (*NST*, ∼35°N) and the *Subtropical Front* (*ST*, ∼30°N), while the *Subarctic Front* (*SA*, ∼42°N) resides within the **SAFZ** (Roden, 1981; Lynn, 1986; Yuan and Talley, 1996). The climatological position of the *SA* is identified in **Figure 2**, while the 2015 location was at 40°N. This offset is discussed in section "Subarctic Frontal Zone and the Subarctic Front Dynamics." The acronyms and locations of fronts/frontal zones described in this manuscript are organized in **Table 1**. For better clarity through this manuscript, frontal zones are written in bold text while individual fronts are italicized.
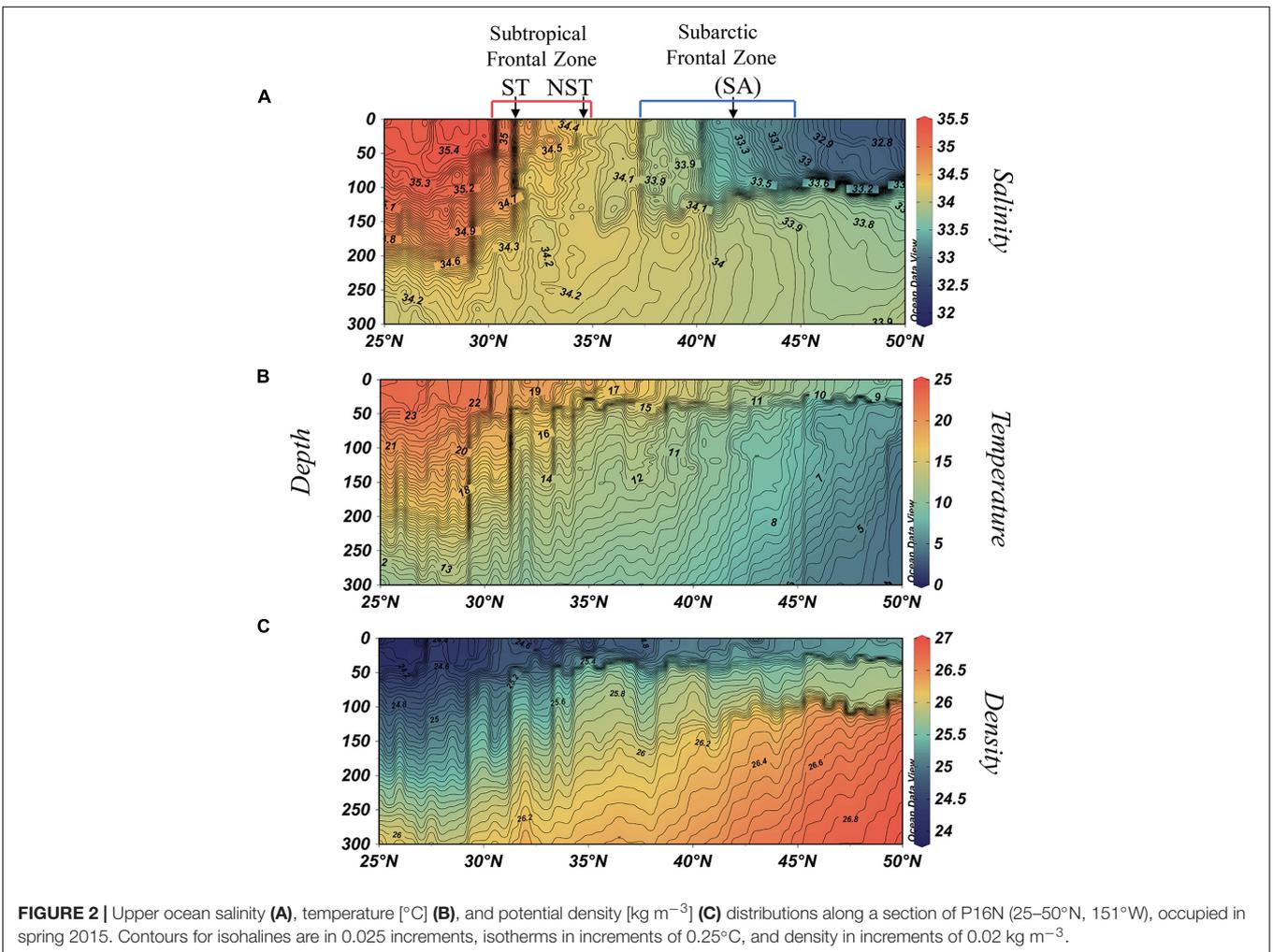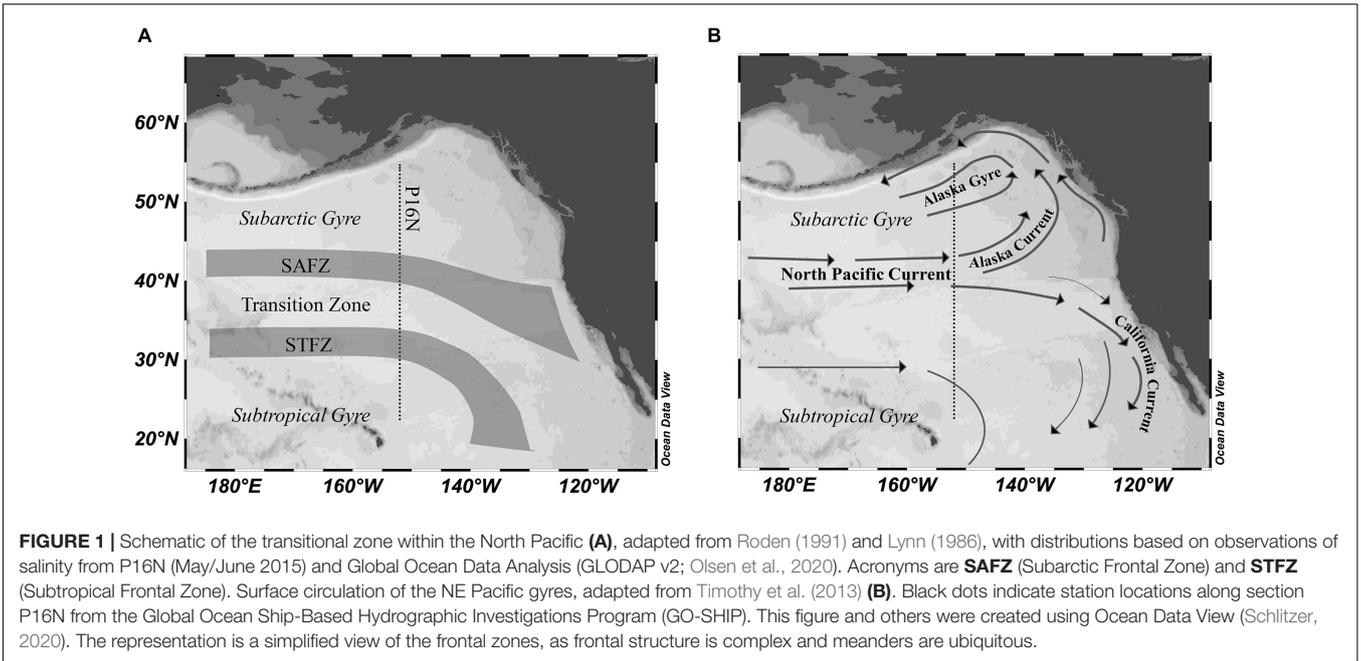
FIGURE 1 | Schematic of the transitional zone within the North Pacific **(A)**, adapted from Roden (1991) and Lynn (1986), with distributions based on observations of salinity from P16N (May/June 2015) and Global Ocean Data Analysis (GLODAP v2; Olsen et al., 2020). Acronyms are **SAFZ** (Subarctic Frontal Zone) and **STFZ** (Subtropical Frontal Zone). Surface circulation of the NE Pacific gyres, adapted from Timothy et al. (2013) **(B)**. Black dots indicate station locations along section P16N from the Global Ocean Ship-Based Hydrographic Investigations Program (GO-SHIP). This figure and others were created using Ocean Data View (Schlitzer, 2020). The representation is a simplified view of the frontal zones, as frontal structure is complex and meanders are ubiquitous.

FIGURE 2 | Upper ocean salinity **(A)**, temperature [°C] **(B)**, and potential density [kg m^{-3}] **(C)** distributions along a section of P16N (25–50°N, 151°W), occupied in spring 2015. Contours for isohalines are in 0.025 increments, isotherms in increments of 0.25°C, and density in increments of 0.02 kg m^{-3}.

	Acronym	Latitude	Salinity
Subarctic Frontal Zone	**SAFZ**	**38–45°N**	**33.0–34.1**
Subarctic Front	*SA*	~41–43°N	33.6
Subtropical Frontal Zone	**STFZ**	**30–35°N**	**34.3–35.2**
Northern Subtropical Front	*NST*	~34°N	34.3
Subtropical Front	*ST*	~31°N	34.8

Frontal zones are shown in bold and individual fronts are italicized.

DISSOLVED ORGANIC CARBON AND PARTICLE DISTRIBUTIONS IN THE BATHYPELAGIC

One important caveat in this analysis: we assign the deep ocean organic carbon concentrations to the DOC fraction, as done in the originating data file (see section "Materials and Methods" and "Data Availability Statement"). Deep water samples collected for organic carbon analysis were whole water at small volumes (100 mL), which is common practice (Carlson et al., 2010). The carbon concentrations are taken to be representative of operationally defined DOC (i.e., organic carbon passing through 0.7 μm filter pores) due to relatively inconsequential particulate organic carbon (POC) concentrations (i.e., on the order of 0.1 μmol kg^{-1} at such great depths; Loh and Bauer, 2000). The DOC and particle abundance distributions (**Figure 3**) are not fully coherent with each other, further suggesting that these whole water organic carbon concentrations are not greatly influenced by optically observable particles.

Returning to the data, we observed two distinct features of elevated DOC concentrations narrowly confined at 34–36°N and 41–43°N (**Figure 3A**) that spanned the entire bathypelagic (>1,000 m). Concentrations at these locations were up to 8 μmol kg^{-1} higher than what is taken as background DOC concentrations in the bathypelagic North Pacific (~36 μmol kg^{-1}; Hansell and Carlson, 2013). Below the subarctic gyre (>45°N), DOC was slightly enriched, from 38 to 40 μmol kg^{-1}. DOC underlying the subtropical gyre was lower, at ~36–38 μmol kg^{-1}.

Dissolved organic carbon concentrations below 1,000 m were segregated by the described frontal/non-frontal regions and are depicted in **Figure 4** The mean DOC concentrations were highest beneath the *NST* and *SA* fronts (40.6 and 40.9 μmol kg^{-1}, respectively) relative to other identified regions (**Table 2**). The lowest mean DOC concentration of 36.9 μmol kg^{-1} was within the subtropical region (25–30°N), followed by the **STFZ** at 37.6 μmol kg^{-1}. The subarctic region (45–50°N) and the **SAFZ** (excluding the *SA*) had similar mean DOC concentrations of 38.8 and 38.6 μmol kg^{-1}, respectively. The range of DOC concentrations within the mid region between the **SAFZ** and **STFZ** was considerably higher than the other zones.

The distribution of particles was segregated into relative size classes: large (>2.05 mm), medium (0.152–2.05 mm), and small (128–152 μm). Each size class had distinctive distributions (**Figures 3B–D**). Small particles were abundant in the bathypelagic from ~36 to 46°N. Abundances of

medium-sized particles were enhanced from ~38 to 43°N. Large particles were most abundant in the bathypelagic at 41–43°N, reaching a maximum of 0.48 particles L^{-1}. A narrow feature of large particles reached the deep ocean at 40°N.

DISCUSSION

Our analysis is focused on the two prominent features of elevated DOC concentrations evident in the water column at ~35°N and ~42°N. We propose these to be residue of export events, such that disaggregation/dissolution of sinking particles was the source of enrichment at such great depth (**Figure 3A**). An allochthonous signal (i.e., introduction by horizontal advection), as an alternative means of introducing the enrichment, would unlikely span the entire water column vertically as observed here; further, a logical distant source region for such enriched waters is not evident in global ocean DOC data (Hansell et al., 2021). Interestingly, the distribution of particles did not completely mirror that of DOC. We explore this dissonance by considering upper ocean dynamics, such as seasonal mixed layer shoaling and regional nutrient access in these distinct frontal zones and their embedded fronts.

Subarctic Frontal Zone and the Subarctic Front Dynamics

One enhanced DOC feature was located beneath the climatological limits of the *SA* (~41–44°N: Yuan and Talley, 1996). Particles of all reported size classes were abundant at this location, but deep export of large particles was uniquely apparent (**Figure 3**). The presence of both enhanced DOC and large particles was not observed elsewhere along the transect.

Enhanced DOC concentrations beneath the climatological *SA* were indicative of deep export; the exported particles likely released DOC into surrounding water during their descent. We conclude that large particles in particular introduced DOC into the bathypelagic, consistent with the current understanding of particle dynamics. Aggregates and larger particles are more abundant in fronts (Ohman et al., 2012) and larger particles are preferentially metabolized by microbes that mediate DOC release (Smith et al., 1992). Our study is also not the first evidence of residue from deep export beneath the *SA*. RuBisCO, a protein tracer for organic matter residue originating from recent export, was similarly elevated throughout the bathypelagic beneath the *SA* in 2006 (Orellana and Hansell, 2012). Mirrored enrichments of RuBisCO reported in 2006 and DOC in 2015, with observations a decade apart, indicate that deep export and its ensuing release of DOC may be a regular process specific to this region.

Stimulating production capable of such deep transport is dependent on frontal mixing in combination with local biogeochemical and hydrographic dynamics such as nutrient availability, MLD, and zooplankton grazing (Franks and Walstad, 1997; Stukel et al., 2017). At the climatological *SA*, we suggest that deep particle export was controlled by frontal mixing into the nutricline. The mixed layer at the *SA* penetrates the nutricline both at its deepest in winter and at its
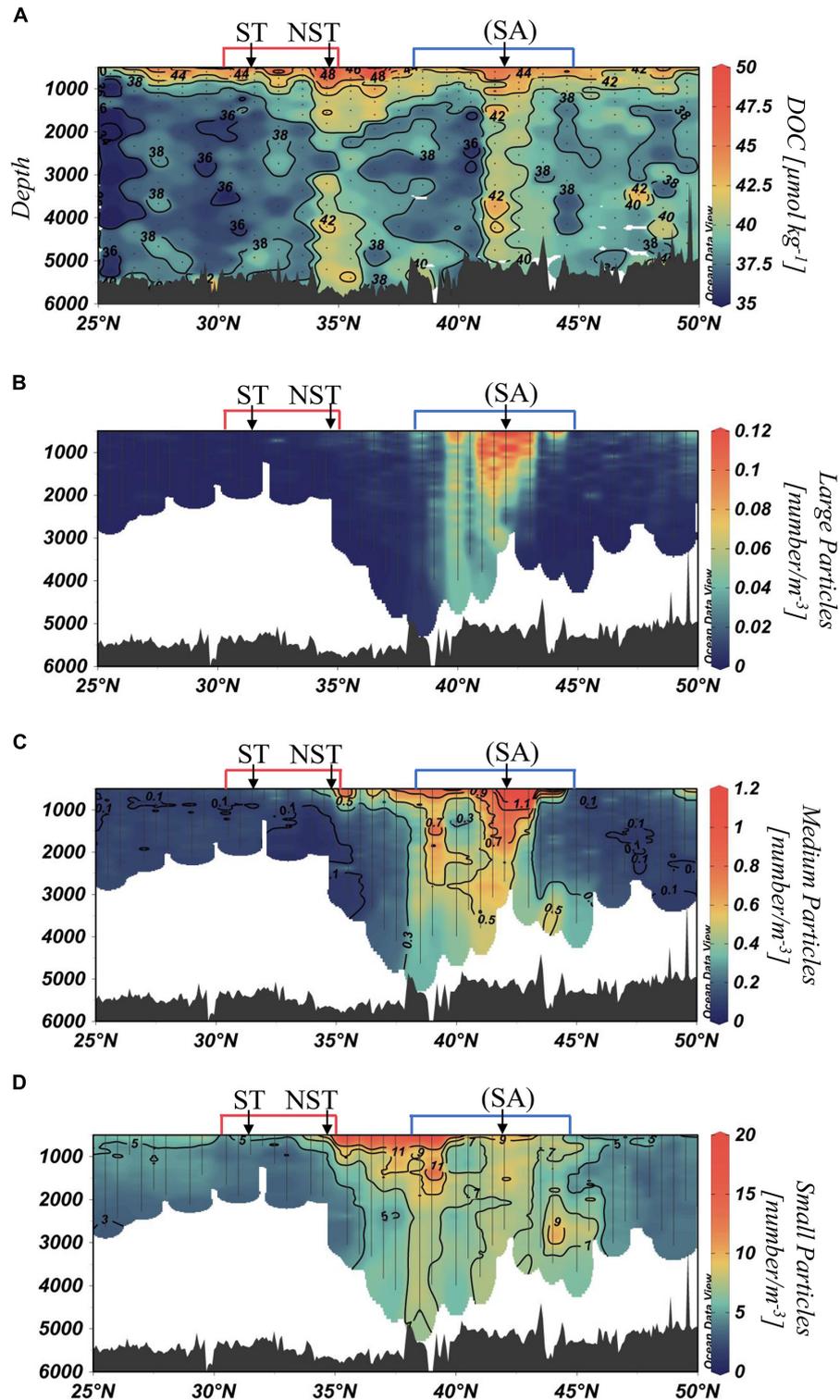
FIGURE 3 | Distributions at >500 m along P16N in spring 2015 of dissolved organic carbon (DOC) [μmol kg^{-1}] **(A)**, large particle abundance of size >2.05 mm [number L^{-1}] **(B)**, medium particle abundance of size 0.512–2.05 mm [number L^{-1}] **(C)**, small particle abundance of size 0.128–0.512 mm [number L^{-1}] **(D)**. The locations of previously described fronts are denoted above each distribution. Red and blue bars indicate locations of the **STFZ** (red) and **SAFZ** (blue). Vertical sample lines represent continuous data from each cast, and dots represent discrete samples. Underwater Vision Profiler (UVP) data have previously been reported by McDonnell and Turner (2016) and Pretty (2019).
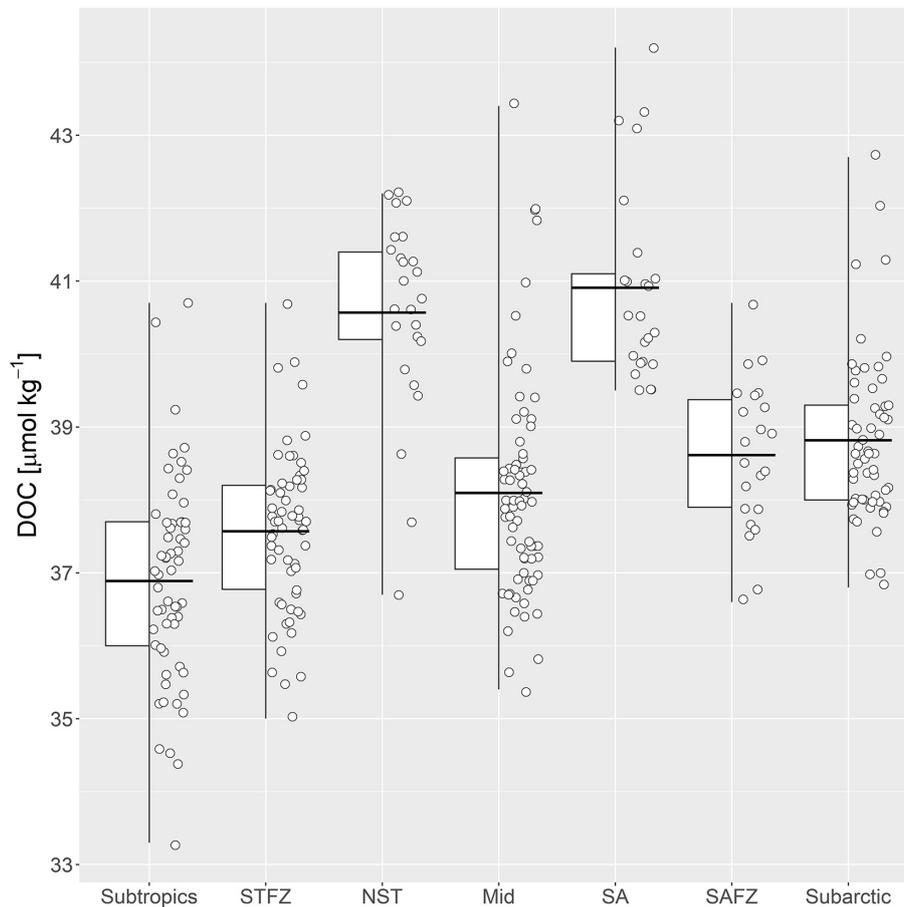
FIGURE 4 | Boxplot of DOC concentrations separated by frontal/non-frontal zones at depths >1,000 m. Dots represent individual measurements within each zone, but their exact position on the *x*-axis is trivial. Whiskers represent the range of DOC concentrations. The lower and upper edges of the boxes represent the first and third quartiles of the data (i.e., 50% of the data lies within the box). The horizontal line represents the mean DOC concentration.

shallowest in spring (**Figure 5**, top panel). This vertical reach provides phytoplankton access to nutrients year-round, thus supporting carbon production and subsequent export. However, the accessibility of nutrients was clearly not the sole factor contributing to favorable conditions for export production. In other regions, studies show that turbulent frontal mixing increases the vertical flux of new nutrients into the euphotic zone, sustaining biological growth to a greater extent than in non-frontal waters (Li et al., 2012; Whitt et al., 2017; Kaneko et al., 2021). It appears that these favorable hydrographic and biogeochemical conditions at the *SA* resulted in deep export of large particles that released DOC.
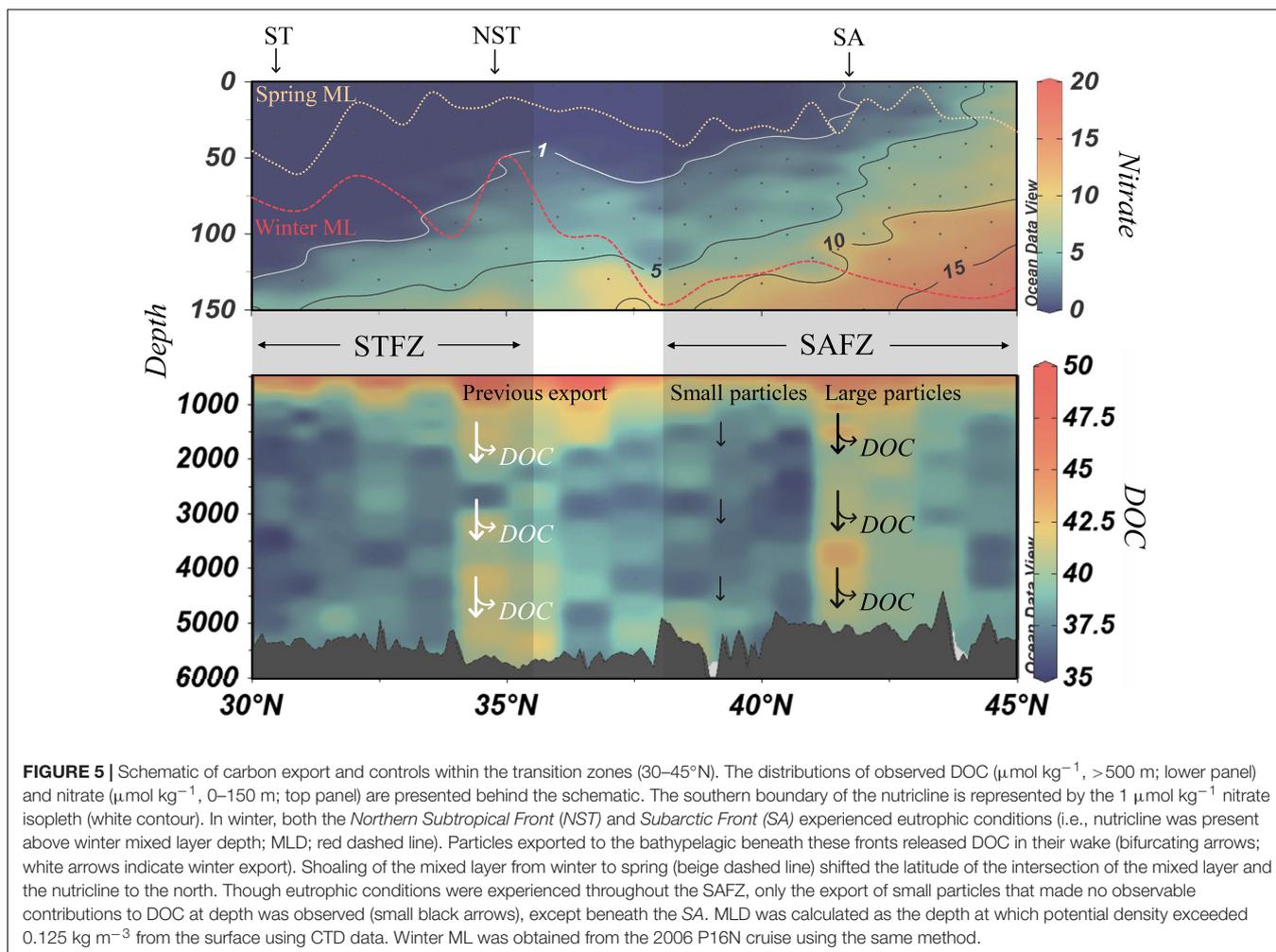
Export was not only observed beneath the *SA*; the entire **SAFZ** exported smaller size classes of particles (<2 mm, **Figures 3C,D**). However, these particles were not associated with enhanced DOC concentrations. Export at these latitudes was unsurprising, as the nutricline is shallow enough throughout the **SAFZ** that winter mixing replenishes nutrients in the euphotic zone to support production (**Figure 5**, upper panel). However, deep export was well restricted within the bounds of the **SAFZ**; intriguing because the mixed layer in the transition zone between the **SAFZ** and

STFZ also reaches the nutricline in winter (**Figure 5**, upper panel), though deep export was not observed. The temporally

TABLE 2 | Dissolved organic carbon (DOC) concentrations of identified frontal/non-frontal zones at depths >1,000 m along 151°W.

		DOC concentration [μmol kg^{-1}]			
	Latitude [°N]	Minimum	Maximum	Range	Mean
Subtropics	25–30	33.3	40.7	7.4	36.9
STFZ*	**30–34***	**35.0**	**40.7**	**5.7**	**37.6**
NST	*34–36*	*36.7*	*42.2*	*5.5*	*40.6*
Mid Region	36–41	35.4	43.4	8.0	38.1
SAFZ*	**33–45***	**35.4**	**40.7**	**4.1**	**38.6**
SA	*41–43*	*39.5*	*44.2*	*4.7*	*40.9*
Subarctic	45–50	36.8	42.7	5.9	38.8

The latitudes are shifted to exclude the embedded Northern Subtropical Front (NST) and Subarctic Front (SA) within the Subtropical Frontal Zone (STFZ) and Subarctic Frontal Zone (SAFZ), respectively. Individual fronts are shown in red. The bold and italics in this table correspond to the previously defined identification system.

FIGURE 5 | Schematic of carbon export and controls within the transition zones (30–45°N). The distributions of observed DOC (μmol kg^{-1}, >500 m; lower panel) and nitrate (μmol kg^{-1}, 0–150 m; top panel) are presented behind the schematic. The southern boundary of the nutricline is represented by the 1 μmol kg^{-1} nitrate isopleth (white contour). In winter, both the *Northern Subtropical Front* (*NST*) and *Subarctic Front (SA)* experienced eutrophic conditions (i.e., nutricline was present above winter mixed layer depth; MLD; red dashed line). Particles exported to the bathypelagic beneath these fronts released DOC in their wake (bifurcating arrows; white arrows indicate winter export). Shoaling of the mixed layer from winter to spring (beige dashed line) shifted the latitude of the intersection of the mixed layer and the nutricline to the north. Though eutrophic conditions were experienced throughout the SAFZ, only the export of small particles that made no observable contributions to DOC at depth was observed (small black arrows), except beneath the *SA*. MLD was calculated as the depth at which potential density exceeded 0.125 kg m^{-3} from the surface using CTD data. Winter ML was obtained from the 2006 P16N cruise using the same method.

variable mesoscale perturbations (i.e., eddies, jets, and transient fronts) that typically exist in the **SAFZ** perhaps stimulated deep export (Franks and Walstad, 1997; Stukel et al., 2017; Resplandy et al., 2019), but without export of the larger particles capable of leaving behind a trace as DOC. Such observations suggest that mixing from quasi-permanent fronts such as the climatological *SA* drive deep, DOC-releasing particle export, while transient perturbations in the **SAFZ** may stimulate deep export of smaller particles that do not leave a trace of DOC.

Further evidence for enhanced export may exist as distinctly elevated dissolved inorganic carbon (DIC) and apparent oxygen utilization (AOU), both products of the cumulative respiration of exported organic material. Salinity-normalized DIC concentrations at depths >3,500 m underlying the **SAFZ** were roughly 10–20 μmol kg^{-1} higher than neighboring waters and AOU was similarly elevated ∼10 μmol kg^{-1} (see **Supplementary Figure 1**). However, the near-bottom waters demonstrating these enrichments were likely introduced with deep anti-cyclonic circulation from the northeast (Reid, 1997), where AOU and DIC are similarly elevated, suggesting that at least part of these signals was imported. These enhancements are also limited to the deep bathypelagic and do not span the

entire vertical water column as we observed with DOC and particle abundances, again suggesting these signals to be a result of advection. Therefore, we cannot discern the extent to which respiration of high particle loads or their byproducts originating from the fronts described here contributed to the enhancement of DIC and AOU, though the linkage likely exists to some degree.

Subtropical Frontal Zone and the Northern Subtropical Front Dynamics

Dissolved organic carbon was also enriched beneath the *NST*, another quasi-permanent front embedded in the **STFZ** (**Figure 3A**). In contrast to the climatological *SA*, enriched DOC was not accompanied by particles of any observed size class (>128 μm). We infer this DOC signal to be residue of export that occurred during the previous winter. If so, particles perhaps were disaggregated into smaller undetectable particles (<128 μm), sedimented onto the seafloor, and/or converted into DOC by spring (the time of observations here). DOC enrichment was the only evidence of deep export within the **STFZ**, as opposed to the **SAFZ** where small particles were observed at depth throughout the zone.

Winter conditions were favorable for phytoplankton growth and ensuing export at the *NST* because (1) the mixed layer easily reached the nutricline and (2) frontal turbulence further enhanced nutrient flux (**Figure 5**, upper panel). However, shoaling of the mixed layer due to development of the seasonal thermocline shifted the latitude at which the mixed layer penetrates the nutricline (i.e., the nitracline) to the north (∼42°N). As a result, oligotrophic conditions stunt production/export since nutrients are not continuously replenished into the mixed layer. Using ocean color imagery, we tracked the seasonal expansion and contraction of eutrophic conditions in this area to better understand this phenomenon, using the position of the Transition Zone Chlorophyll Front (TZCF) as our metric. The TZCF marks the southernmost latitude at which eutrophic conditions exist, with oligotrophic conditions to its south. This boundary migrates seasonally, lying furthest south in winter (Polovina et al., 2001, 2017). In winter 2015, the TZCF was at 34°N, its southernmost reach, and co-located with the southern boundary of the *NST*, indicating that eutrophic conditions made production at these latitudes favorable (**Figure 6A**). The TZCF, and thus eutrophic conditions, shifted northward to ∼42°N by spring (**Figures 6B,C**), no longer encompassing the *NST*. Presumably export at the *NST* ceased with the loss of eutrophic conditions, yet DOC remained enriched at great depth.

Also embedded in the **STFZ** is the *ST*, though no indication of recent or previous deep export was evident there (i.e., absence of both particles and DOC enrichment at depth). Since the mixed layer does not reach the nutricline during any season at the *ST* (**Figure 5**, upper panel), the euphotic zone at the front apparently lacks the conditions necessary to sustain elevated phytoplankton growth.
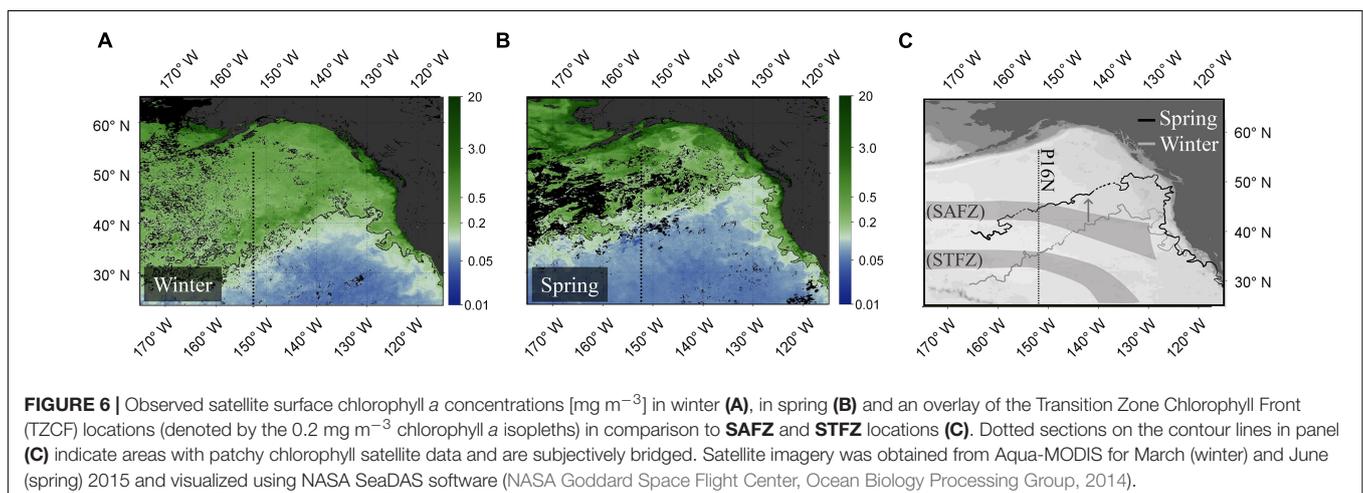
FURTHER CONSIDERATIONS

Though these observations advance our understanding of export dynamics across a prominent frontal region, the ocean is undeniably variable in time and space and we must be careful not to oversimplify the transitional region. One such consideration is the interannual variability of the TZCF, and thus the shift of eutrophic conditions. The TZCF has been located further south in the past (Bograd et al., 2004), pushing eutrophic conditions further into the subtropics and within the **STFZ**. As such, deep carbon export and enhancement of DOC may occur in the **SAFZ** and *STF* in other years. El Niño and La Niña events also affect the location and migration of the TZCF (Bograd et al., 2004) and southward shifts of fronts due to strengthened westerlies during El Niño have been reported (Roden, 1991; Bograd et al., 2004). Since 2015 was an exceptionally strong El Niño year (Null, 2021), the observations we report here may be entirely different to what we might observe in a La Niña or neutral year. Previous studies have considered El Niño's effect on production within a front in the equatorial Pacific, noting ∼50% less production during El Niño (Honjo et al., 2008), demonstrating the potential for significant fluctuations in production as a response to climate modes.

We found that the latitude of the *SA* during 2015 was anomalously located at 40°N, outside its climatological bounds of 41–43°N (**Figure 2A**, 33.6 salinity outcrop) (Yuan and Talley, 1996). As mentioned above, 2015 was a strong El Niño year and we suspect that the *SA* was consequentially shifted to the south. Deep export at the actual location of the *SA* in 2015 was apparent as a narrow signal of large particles (**Figure 3B**). However, DOC was not elevated like it was at the climatological range of the *SA*, suggesting that deep particle export from the actual *SA* was not instantly releasing DOC. As such, deep export at 40°N likely does not occur in most years, thus providing serendipitous evidence for the temporal nature of DOC enhancements beneath the climatological *SA*. The signal there may result from accumulation since DOC is enhanced within the latitudinal range of the climatological *SA* but not at the location of the actual *SA* in 2015. However, we do not know the timescale of such DOC accumulation in this unique area, whether it be seasonal, interannual, or longer.

The zonal variability of both the TZCF and the physical fronts should also be considered, as the locations of the frontal zones we report here relative to the TZCF is specific to this

FIGURE 6 | Observed satellite surface chlorophyll *a* concentrations [mg m^{-3}] in winter **(A)**, in spring **(B)** and an overlay of the Transition Zone Chlorophyll Front (TZCF) locations (denoted by the 0.2 mg m^{-3} chlorophyll *a* isopleths) in comparison to **SAFZ** and **STFZ** locations **(C)**. Dotted sections on the contour lines in panel **(C)** indicate areas with patchy chlorophyll satellite data and are subjectively bridged. Satellite imagery was obtained from Aqua-MODIS for March (winter) and June (spring) 2015 and visualized using NASA SeaDAS software (NASA Goddard Space Flight Center, Ocean Biology Processing Group, 2014).

longitude. It may be the case that the **STFZ**/*SF* experiences eutrophic conditions elsewhere in the basin. In addition, the fronts discussed in this manuscript are notably stronger in the western Pacific (Yuan and Talley, 1996), resulting in deeper mixing and likely higher vertical nutrient flux than the central and eastern Pacific. It is possible that these fronts stimulate more export in the western Pacific and therefore transfer additional DOC to the deep ocean in those locations.

The apparent focus of large particle export and its enrichment of DOC at great depth at major fronts is likely impacting the deep microbe community in very direct ways (Ruiz-González et al., 2020). For example, large particle export is an important mechanism for the vertical dispersal of prokaryotes, connecting surface communities to those in the dark ocean (Mestre et al., 2018). Thus, the enhancement of export at the fronts may shape the local biogeography of the deep prokaryotic communities. If distinct microbial communities are indeed located below the fronts, they are likely sustained by the DOC released from these particles. Smith et al. (1992) described the hydrolysis of sinking particles as the biochemical mechanism for the large-scale transfer of organic matter from the particulate to dissolved phases, a process supporting deep microbes as inferred from their distributions in the deep ocean (Nagata et al., 2000; Hansell and Ducklow, 2003). Baltar and Arístegui (2017) noted the important role of permanent ocean fronts as ecological boundaries for bathypelagic microbial community structure and biogeochemical cycling. A higher resolution evaluation of the boundaries themselves should be made; the microbial dynamics there may represent an end member for the deep ocean.

CONCLUSION

Hydrographic fronts within the transitional zone between the subarctic and subtropical gyres of the North Pacific appear to be unique drivers for the introduction of DOC to great depths *via* deep-sinking particles. By analyzing DOC distributions below important hydrographic frontal zones, in combination with nutrient distributions, particle abundances, and satellite chlorophyll imagery, we conclude:

(1) Dissolved organic carbon introduction *via* particle export into the bathypelagic occurred at the *NST* and *SA*.
(2) An enhancement of deep DOC beneath the *NST* was inferred to be residue of export that occurred in the preceding winter. Export did not continue in spring because eutrophic conditions shifted northward.
(3) Hydrographic and biogeochemical conditions in the **SAFZ** stimulated deep particle export. However, it is apparent that mixing from strong quasi-permanent fronts alone resulted in particle export capable of releasing DOC.
(4) Dissolved organic carbon introduction beneath fronts was dependent on both the presence of a strong physical front and access to the nutricline.

These observations reveal that fronts within suitable biogeochemical environments induce deep carbon export capable of enriching DOC. Such findings indicate that the transitional region of the North Pacific, and perhaps analogous systems in other ocean basins, may be major contributors of carbon export and sustenance for deep microbial populations.

MATERIALS AND METHODS

Hydrographic data (salinity, temperature, density, and nitrate) and DOC concentrations included in this analysis were collected from transect P16N (25–50°N) in May/June of 2015 as part of GO-SHIP (Macdonald and Mecking, 2020). We report DOC concentrations at >500 m only as the focus here is on deep export. Samples were collected directly from Niskin bottles into high-density polyethylene (HDPE) bottles and thawed and acidified immediately before analysis. The contribution of organic carbon from particles at depths >500 m is assumed to be inconsequential. Samples were analyzed with Shimadzu TOC-L systems. Reference materials from the Certified Reference Material (CRM) program (Hansell, 2005) were utilized to ensure accuracy. The uncertainty of DOC measurements is $\pm 1.5 \mu$mol L^{-1}.

Particle size classes have been subjectively segregated into small (128–512 μm), medium (512 μm – 2.05 mm), and large (>2.05 mm). Particle data and distributions shown here were previously reported by McDonnell and Turner (2016) and Pretty (2019).

For more detailed methods information for all variables considered here, visit https://cchdo.ucsd.edu/.

DATA AVAILABILITY STATEMENT

Satellite data were obtained from the Ocean Biology Processing Group (OBPG), available at https://oceancolor.gsfc.nasa.gov/. Underwater Vision Profiler (UVP) data were obtained from EcoTaxa (https://ecotaxa.obs-vlfr.fr/) for project uvp5 sn009 2015 p16n (Picheral et al., 2017). Size classes smaller than 128 μm are not reported in this analysis, as measurements of particles beneath this size class become less accurate (Picheral et al., 2010; Turner et al., 2017). CTD, nutrient and DOC data are available from the Carbon Hydrographic Data Office (CCHDO) at https://cchdo.ucsd.edu/ for cruise 33RO20150525 (P16N).

AUTHOR CONTRIBUTIONS

CL and DH conceived the idea and designed the project. CL completed the data analysis and wrote the manuscript. Both authors contributed to the article and approved the submitted version.

FUNDING

ACKNOWLEDGMENTS

SUPPLEMENTARY MATERIAL

The Supplementary Material for this article can be found online at: https://www.frontiersin.org/articles/10.3389/fmars.2021.659034/full#supplementary-material

REFERENCES

Alldredge, A. L., Granata, T. C., Gotschalk, C. C., and Dickey, T. D. (1990). The physical strength of marine snow and its implications for particle disaggregation in the ocean. *Limnol. Oceanogr.* 35, 1415–1428. doi: 10.4319/lo.1990.35.7.1415

Baltar, F., and Arístegui, J. (2017). Fronts at the surface ocean can shape distinct regions of microbial activity and community assemblages down to the bathypelagic zone: the azores front as a case study. *Front. Mar. Sci.* 4:252. doi: 10.3389/fmars.2017.00252

Bograd, S., Foley, D., Schwing, F., Wilson, C., Laurs, R., Polovina, J., et al. (2004). On the seasonal and interannual migrations of the transition zone chlorophyll front. *Geophys. Res. Lett.* 31:L17204. doi: 10.1029/2004GL020637

Carlson, C. A., Hansell, D. A., Nelson, N. B., Siegel, D. A., Smethie, W. M., Khatiwala, S., et al. (2010). Dissolved organic carbon export and subsequent remineralization in the mesopelagic and bathypelagic realms of the North Atlantic basin. *Deep-Sea Res. II* 57, 1433–1445.

D'Asaro, E., Lee, C., Rainville, L., Harcourt, R., and Thomas, L. (2011). Enhanced turbulence and energy dissipation at ocean fronts. *Science* 332, 318–322. doi: 10.1126/science.1201515

Franks, P. J. S., and Walstad, L. J. (1997). Phytoplankton patches at fronts: a model of formation and response to wind events. *J. Mar. Res.* 55, 1–29. doi: 10.1357/0022240973224472

Guidi, L., Calil, P. H. R., Duhamel, S., Björkman, K. M., Doney, S. C., Jackson, G. A., et al. (2012). Does eddy-eddy interaction control surface phytoplankton distribution and carbon export in the north pacific subtropical gyre? *J. Geophys. Res. Biogeosci.* 117:G02024. doi: 10.1029/2012JG001984

Hansell, D. A. (2005). Dissolved organic carbon reference material program. *Eos Transact. Am. Geophys. Union* 86:318. doi: 10.1029/2005EO350003

Hansell, D. A., and Carlson, C. A. (2013). Localized refractory dissolved organic carbon sinks in the deep ocean. *Glob. Biogeochem. Cycles* 27, 705–710. doi: 10.1002/gbc.20067

Hansell, D. A., Carlson, C. A., Amon, R. M. W., Álvarez-Salgado, X., Yamashita, Y., Romera-Castillo, C., et al. (2021). *Compilation of Dissolved Organic Matter (DOM) Data Obtained from the Global Ocean Surveys From 1994 to 2020 (NCEI Accession 0227166). NOAA National Centers for Environmental Information.* Available online at: doi.org/10.25921/s4f4-ye35 (accessed June 1, 2021).

Hansell, D. A., and Ducklow, H. W. (2003). Bacterioplankton distribution and production in the bathypelagic ocean: directly coupled to particulate organic carbon export? *Limnol. Oceanogr.* 48, 150–156. doi: 10.4319/lo.2003.48.1.0150

Honjo, S., Manganini, S. J., Krishfield, R. A., and Francois, R. (2008). Particulate organic carbon fluxes to the ocean interior and factors controlling the biological pump: a synthesis of global sediment trap programs since 1983. *Prog. Oceanogr.* 76, 217–285. doi: 10.1016/j.pocean.2007.11.003

Howell, E. A., Bograd, S. J., Hoover, A. L., Seki, M. P., and Polovina, J. J. (2017). Variation in phytoplankton composition between two north pacific frontal zones along 158°W during winter–spring 2008–2011. *Prog. Oceanogr.* 150, 3–12. doi: 10.1016/j.pocean.2015.06.003

Juranek, L. W., Quay, P. D., Feely, R. A., Lockwood, D., Karl, D. M., and Church, M. J. (2012). Biological production in the NE pacific and its influence on air-sea CO_2 flux: evidence from dissolved oxygen isotopes and O_2/Ar. *J. Geophys. Res. Oceans* 117:C05022. doi: 10.1029/2011JC007450

Kaneko, H., Yasuda, I., Itoh, S., and Ito, S-i (2021). Vertical turbulent nitrate flux from direct measurements in the Western subarctic and subtropical gyres of the North Pacific. *J. Oceanogr.* 77, 29–44. doi: 10.1007/s10872-020-00576-0

Käse, R. H., Zenk, W., Sanford, T. B., and Hiller, W. (1985). Currents, fronts and eddy fluxes in the Canary Basin. *Prog. Oceanogr.* 14, 231–257. doi: 10.1016/0079-6611(85)90013-8

Kobari, T., Honma, T., Hasegawa, D., Yoshie, N., Tsutsumi, E., Matsuno, T., et al. (2020). Phytoplankton growth and consumption by microzooplankton stimulated by turbulent nitrate flux suggest rapid trophic transfer in the oligotrophic kuroshio. *Biogeosciences* 17, 2441–2452. doi: 10.5194/bg-17-2441-2020

Li, Q. P., Franks, P. J. S., Ohman, M. D., and Landry, M. R. (2012). Enhanced nitrate fluxes and biological processes at a frontal zone in the southern california current system. *J. Plankton Res.* 34, 790–801. doi: 10.1093/plankt/fbs006

Lockwood, D., Quay, P. D., Kavanaugh, M. T., Juranek, L. W., and Feely, R. A. (2012). High-resolution estimates of net community production and air-sea CO_2 flux in the Northeast Pacific. *Glob. Biogeochem. Cycles* 26:GB4010. doi: 10.1029/2012GB004380

Loh, A. N., and Bauer, J. E. (2000). Distribution, partitioning and fluxes of dissolved and particulate organic C, N and P in the Eastern North Pacific and Southern oceans. *Deep Sea Res. Part I Oceanogr. Res. Papers* 47, 2287–2316. doi: 10.1016/S0967-0637(00)00027-3

Lopez, C. N., Robert, M., Galbraith, M., Bercovici, S. K., Orellana, M. V., and Hansell, D. A. (2020). High temporal variability of total organic carbon in the deep Northeastern Pacific. *Front. Earth Sci.* 8:80. doi: 10.3389/feart.2020.00080

Lynn, R. J. (1986). The subarctic and northern subtropical fronts in the eastern North Pacific Ocean in spring. *J. Phys. Oceanogr.* 16, 209–222.

Macdonald, A., and Mecking, S. (2020). *CTD/Bottle Data From Cruise 33RO20150525, Exchange Version.* Available online at: https://cchdo.ucsd.edu/cruise/33RO20150525 (accessed March 01, 2020).

McDonnell, A. M. P., and Turner, J. S. (2016). Large-scale patterns and drivers of the biological carbon pump: insights from in situ camera observations across the Pacific Ocean. *Ocean Sci. Meeting* 2016, 21A–23A.

Mestre, M., Ruiz-González, C., Logares, R., Duarte, C. M., Gasol, J. M., and Sala, M. M. (2018). Sinking particles promote vertical connectivity in the ocean microbiome. *Proc. Natl. Acad. Sci. U.S.A.* 115, E6799–E6807. doi: 10.1073/pnas.1802470115

Nagata, T., Fukuda, H., Fukuda, R., and Koike, I. (2000). Bacterioplankton distribution and production in deep pacific waters: large-scale geographic variations and possible coupling with sinking particle fluxes. *Limnol. Oceanogr.* 45, 426–435. doi: 10.4319/lo.2000.45.2.0426

Nagata, T., Tamburini, C., Arístegui, J., Baltar, F., Bochdansky, A. B., Fonda-Umani, S., et al. (2010). Emerging concepts on microbial processes in the bathypelagic ocean – ecology, biogeochemistry, and genomics. *Deep Sea Res. Part II Top. Stud. Oceanogr.* 57, 1519–1536. doi: 10.1016/j.dsr2.2010.02.019

Nakamura, H., Sampe, T., Goto, A., Ohfuchi, W., and Xie, S.-P. (2008). On the importance of midlatitude oceanic frontal zones for the mean state and dominant variability in the tropospheric circulation. *Geophys. Res. Lett.* 35:L15709. doi: 10.1029/2008GL034010

NASA Goddard Space Flight Center, Ocean Biology Processing Group (2014). *Sea-Viewing Wide Field-of-View SENSOR (SeaWiFS) Ocean Color Data.* Greenbelt, MD: NASA OB.DAAC.

Null, J. (2021). *El Niño and La Niña Years and Intensities.* Saratoga, CA: Golden Gate Weather Services.

Ohman, M. D., Powell, J. R., Picheral, M., and Jensen, D. W. (2012). Mesozooplankton and particulate matter responses to a deep-water frontal system in the Southern California current system. *J. Plankton Res.* 34, 815–827. doi: 10.1093/plankt/fbs028

Olsen, A., Lange, N., Key, R., Tanhua, T., Bittig, H., Kozyr, A., et al. (2020). GLODAPv2.2020 – the second update of GLODAPv2. *Oceanogr. Chem.* doi: 10.5194/essd-2020-165

Orellana, M. V., and Hansell, D. A. (2012). Ribulose-1,5-bisphosphate carboxylase/oxygenase (RuBisCO): a long-lived protein in the deep ocean. *Limnol. Oceanogr.* 57, 826–834. doi: 10.4319/lo.2012.57.3.0826

Pearcy, W. G. (1991). "Biology of the transition region. 1991," in *Biology, Oceanography, and Fisheries of the North Pacific Transition Zone and Subarctic Frontal Zone. Hon. Lab, SWFSC, Nat. Mar. Fish. Ser. Tech. Rpt.* NOAA Technical Report NMFS, Vol. 105, ed. J. A. Wetherall (Washington, DC: NOAA), 1–38.

Picheral, M., Colin, S., and Irisson, J.-O. (2017). *EcoTaxa, A Tool for the Taxonomic Classification of Images*. Available online at: http://ecotaxa.obs-vlfr (accessed February 15, 2020).

Picheral, M., Guidi, L., Stemmann, L., Karl, D. M., Iddaoud, G., and Gorsky, G. (2010). The underwater vision profiler 5: an advanced instrument for high spatial resolution studies of particle size spectra and zooplankton: underwater vision profiler. *Limnol. Oceanogr. Methods* 8, 462–73. doi: 10.4319/lom.2010.8.462

Polovina, J. J., Howell, E., Kobayashi, D. R., and Seki, M. P. (2001). The transition zone chlorophyll front, a dynamic global feature defining migration and forage habitat for marine resources. *Prog. Oceanogr.* 49, 469–483. doi: 10.1016/S0079-6611(01)00036-2

Polovina, J. J., Howell, E., Kobayashi, D. R., and Seki, M. P. (2017). The transition zone chlorophyll front updated: advances from a decade of research. *Prog. Oceanogr.* 150, 79–85. doi: 10.1016/j.pocean.2015.01.006

Pretty, J. (2019). *Particles in the Pacific: How Productivity and Zooplankton Relate to Particles in the Deep Sea*. Master's thesis. Fairbanks, AK: University of Alaska Fairbanks.

Reid, J. L. (1997). On the total geostrophic circulation of the pacific ocean: flow patterns, tracers, and transports. *Prog. Oceanogr.* 39, 263–352. doi: 10.1016/S0079-6611(97)00012-8

Resplandy, L., Lévy, M., and McGillicuddy, D. J. (2019). Effects of Eddy? Driven subduction on ocean biological carbon pump. *Glob. Biogeochem. Cycles* 33, 1071–1084. doi: 10.1029/2018GB006125

Roden, G. I. (1970). Aspects of the mid-pacific transition zone. *J. Geophys. Res.* 75, 1097–1109. doi: 10.1029/JC075i006p01097

Roden, G. I. (1980). On the subtropical frontal zone North of Hawaii during winter. *J. Phys. Oceanogr.* 10, 342–362.

Roden, G. I. (1981). Mesoscale thermohaline, sound velocity, and baroclinic flow structure of the Pacific Subtropical Front during the winter of 1980. *J. Phys. Oceanogr.* 11, 658–675.

Roden, G. I. (1991). "Subarctic-subtropical transition zone of the North Pacific: largescale aspects and mesoscale structure," in *Biology, Oceanography, and Fisheries of the North Pacific Transition Zone and Subarctic Frontal Zone. Hon. Lab, SWFSC, Nat. Mar. Fish. Ser. Tech. Rpt.* NOAA Technical Report NMFS , Vol. 105, ed. J. A. Wetherall (Washington, DC: NOAA), 1–38.

Ruiz-González, C., Mestre, M., Estrada, M., Sebastián, M., Salazar, G., Agustí, S., et al. (2020). Major imprint of surface plankton on deep ocean prokaryotic structure and activity. *Mol. Ecol.* 29, 1820–1838. doi: 10.1111/mec.15454

Schlitzer, R. (2020). *Ocean Data View*. Available online at: odv.awi.de (accessed March 2, 2021).

Smith, D., Simon, M., Alldredge, A., and Farooq, A. (1992). Intense hydrolytic enzyme activity on marine aggregates and implications for rapid particle dissolution. *Nature* 359, 139–142. doi: 10.1038/359139a0

Stukel, M. R., Aluwihare, L. I., Barbeau, K. A., Chekalyuk, A. M., Goericke, R., Miller, A. J., et al. (2017). Mesoscale ocean fronts enhance carbon export due to gravitational sinking and subduction. *Proc. Natl. Acad. Sci. U.S.A.* 114, 1252–1257. doi: 10.1073/pnas.1609435114

Timothy, D. A., Wong, C. S., Barwell-Clarke, J. E., Page, J. S., White, L. A., and Macdonald, R. W. (2013). Climatology of sediment flux and composition in the subarctic northeast pacific ocean with biogeochemical implications. *Progr. Oceanogr.* 116, 95–129. doi: 10.1016/j.pocean.2013.06.017

Turner, J. S., Pretty, J. L., and McDonnell, A. M. P. (2017). Marine particles in the Gulf of Alaska shelf system: spatial patterns and size distributions from in situ optics. *Continent. Shelf Res.* 145, 13–20. doi: 10.1016/j.csr.2017.07.002

Whitt, D. B., Taylor, J. R., and Lévy, M. (2017). Synoptic-to-planetary scale wind variability enhances phytoplankton biomass at ocean fronts. *J. Geophys. Res. Oceans* 122, 4602–4633. doi: 10.1002/2016JC011899

Woodson, C. B., and Litvin, S. Y. (2015). Ocean fronts drive marine fishery production and biogeochemical cycling. *Proc. Natl. Acad. Sci. U.S.A.* 112, 1710–1715. doi: 10.1073/pnas.1417143112

Yuan, X., and Talley, L. D. (1996). The subarctic frontal zone in the North Pacific: characteristics of frontal structure from climatological data and synoptic surveys. *J. Geophys. Res. Oceans* 101, 16491–16508. doi: 10.1029/96JC01249